Shape memory through contact: Introduction of MagnetoFriction – Shape Memory Polymers (MF-SMPs)

Svenja Hermann, Gaël Chevallier, Laurent Hirsinger, Morvan Ouisse

Shape Memory through Contact : Introduction of Magnetofriction – Shape Memory Polymers (MF-SMPs)

S. HERMANN[a], G. CHEVALLIER[a], L. HIRSINGER[b], M. OUISSE[a]

Institut FEMTO-ST, CNRS/UFC/ENSMM/UTBM/UBFC, F-25000 Besançon, France
a. Département Mécanique Appliquée
b. Département Micro Nano Sciences et Systèmes
Contact : gael.chevallier@univ-fcomte.fr or svenja.hermann@femto-st.fr

Résumé :

Ce travail introduit un nouveau concept pour la mémoire de forme dans les structures composites assemblées. Ce concept, appelé magnétofriction, est basé sur le magnétisme, l'élasticité, le contact et le frottement. Dans les assemblages d'Élastomères Magnétoactifs (MAE), aimantés de façon permanente, la pression de contact est établie par des forces d'attraction d'origine magnétique. Lorsque l'assemblage est déformé, les surfaces en contact glissent l'une sur l'autre et la forme déformée est ensuite verrouillée par la friction dans l'interface. Un relâchement du contact fait disparaître les forces de friction et chaque partie de l'assemblage retrouve son état initial grâce aux forces élastiques des matériaux. Le contact peut être rétabli quand les pièces ont récupéré leur forme initiale. Un assemblage de test, appelé MagnétoFriction - Polymère à Mémoire de Forme (MF-PMF), est utilisé pour valider le concept expérimentalement. Le glissement local et le verrouillage de la forme sont observés dans les tests de flexion en trois points ce qui prouve le concept de magnétofriction. Deux solutions pour la récupération de la forme initiale sont proposées. Par ailleurs, la magnétofriction est comparée à d'autres mécanismes pour classer ce nouveau concept dans le domaine des matériaux à mémoire de forme.

Abstract :

This work introduces a new, multi-physical concept for shape memory in assembled composite structures. The concept is called magnetofriction and is based on magnetism, elasticity, contact and friction. In assemblies of permanently magnetized Magnetoactive Elastomers (MAE), the contact pressure is established by magnetic attraction forces. When the assembly is deformed, the contact surfaces slide over each other and the deformed shape is locked by the friction in the interface. A loosening of the contact causes the friction forces to vanish and each part of the assembly recovers its initial state due to the elastic forces in the materials. The contact is restored after the shape recovery. A test assembly, called Magnetofriction – Shape Memory Polymer (MF-SMP), is used to validate the concept experimentally. A local sliding and a shape lock are observed in three-point bending tests which proves the concept of magnetofriction. Furthermore, two solutions for the shape recovery are proposed. Magnetofriction is compared to other mechanisms to classify the new concept in the field of shape memory materials.

Mots clefs : Shape memory, magnetoactive elastomer (MAE), assembled structure, magnetic attraction forces, contact pressure, friction

1 Introduction

The term “Shape Memory Effect” describes the ability of a material or a structure to alter its shape between different stable states as a response to external stimuli. At least one stable state is memorized by the system [1]. Possible applications for the shape memory effect can be found in the field of actuators, where different stable states can be used to maintain positions without an external energy supply [2, 3]. Furthermore, a controlled repetitive shape change has been used in the field of soft robots to achieve different modes of locomotion [4] and to design biomedical applications [5].

The shape memory effect can be triggered by different physical stimuli in different types of materials. Two well-known activation stimuli are a mechanical loading and a temperature variation which are applied to control Shape Memory Alloys (SMAs) for example. SMAs are capable to recover seemingly permanent strains when heated due to a phase transformation between two stable phases : martensite and austenite [6]. The application of mechanical stresses to the low temperature martensite phase causes a reorientation from a twinned to a detwinned state. Heating the material results in a phase transformation into the austenite phase, whereby the strain is recovered. After cooling, the SMA recovers its twinned martensite state [7].

The shape memory of thermally activated Shape Memory Polymers (SMPs) is based on the phase transition between the rubbery and the glassy state [8, 9]. After the cooling, SMPs memorize the deformation previously applied in the high temperature state. The recovery of the initial shape is activated by the application of temperatures above the glass transition temperature [10]. To activate the shape memory without heating the environment of SMPs, recent works propose to embed magnetic particles in the polymer and use inductive heating of Magnetic (M-)SMPs for the phase transition [11, 12].

In Magnetic Shape Memory Alloys (M-SMAs), a shape change can be achieved by external magnetic fields due to the reorientation of martensite [2]. The magnetic shape memory effect in M-SMAs is temperature dependent [13]. Permanently magnetized magnetically Hard Magnetoactive Elastomers (H-MAEs) can also show a shape memory effect in presence of external magnetic fields [14, 15]. The shape change occurs when the H-MAE presents regions with different orientations of the magnetic moments that align with external magnetic fields. When the external field is switched off, the elastic forces bring the H-MAE back to its initial shape.

The activation of the phase transitions are generally slow and a temperature hysteresis has to be considered in thermally activated shape memory materials. While the deformation capacity of M-SMAs is comparatively low due to the stiffness of the material, H-MAEs need to be surrounded by a magnetic field constantly to stay in the deformed configuration. The new concept for shape memory, presented in Section 2 of this study, aims to overcome some of the challenges in existing shape memory materials by using friction instead of a phase change to achieve shape memory. The storage of a deformed shape is studied in detail in Section 3 and two solutions for the recovery of the initial shape are presented in Section 4. In Section 5 magnetofriction is compared to other shape memory mechanisms.

2 Shape memory by magnetofriction

2.1 Concept

The concept for shape memory in this work is based on the competing strength of elastic forces and magnetically induced friction forces. Friction forces occur in the contact interfaces of assembled structures. They depend on the contact pressure which maintains the assembly together. In a Magnetofriction - Shape Memory Polymer (MF-SMP), the contact pressure is established magnetically. An MF-SMP is assembled from permanently magnetized H-MAEs. Due to the magnetization, magnetic attraction forces develop between the H-MAEs. The magnetic forces establish the pressure in the contact interface that maintains the MF-SMP assembled (Fig. 1, “Initial, stable state").

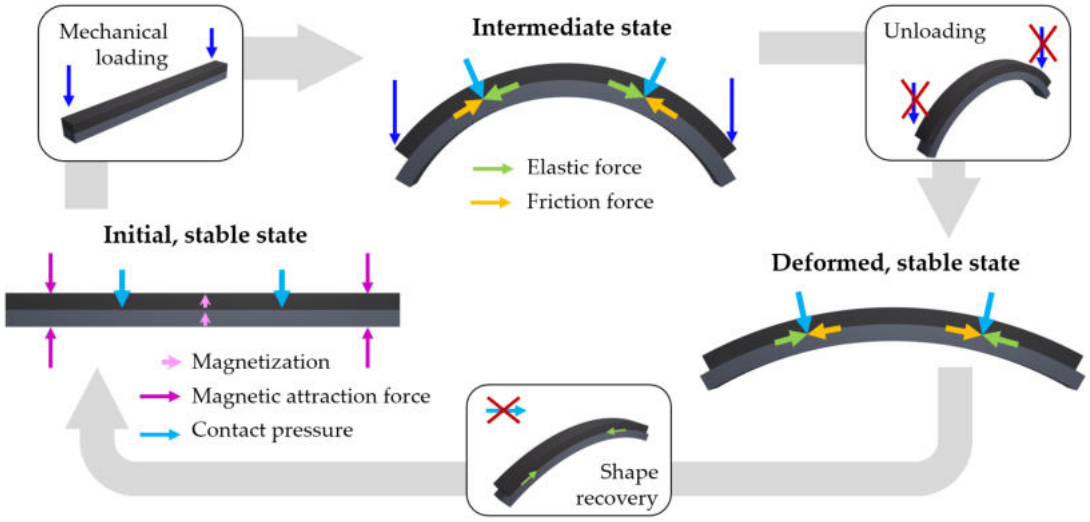

Figure 1 – Illustration of the deformation cycle of a Magnetofriction Shape Memory Polymer (MF-SMP) assembled from two magnetized magnetically hard magnetoactive elastomers.

The H-MAEs are elastic and have a low mechanical stiffness. The assembled MF-SMP can hence easily be deformed. When the assembly is deformed, elastic stresses appear in the material and generate constraints in the interface. According to Coulomb’s friction law, friction forces maintain the adhesion between two points of the contact interface up to a specific threshold that depends on the material pairing. When the elastic constraints in the H-MAEs generate forces in the interface that exceed the friction forces, the contact surfaces slide over each other. The sliding releases a part of the elastic constraints in the assembly. As the elastic constraints in the interface are decreased by the sliding, the contact state changes from sliding to adhesion. The H-MAEs stick together once again due to the magnetically induced contact pressure (Fig. 1, “Intermediate state").

When the mechanical loading is released, the elastic forces tend to bring each H-MAE back to its initial shape. They deform the MF-SMP and also generate restoring forces in the contact interface. In the interface, however, the restoring forces have to work against the friction forces. As a result, only a part of the applied deformation is restored as long as the friction forces are present (Fig. 1, “Deformed, stable state"). When the magnetic attraction forces disappear, the friction forces vanish and the elastic

forces bring the parts of the assembly back into their initial shape. The restoring of the contact pressure completes the shape memory cycle.

2.2 Design of a Magnetofriction Shape Memory Polymer

To prove the concept of magnetofriction a test structure is assembled from two H-MAE beams. The H-MAE in this study consists of 36 vol % NdFeB particles which are randomly dispersed in a silicone matrix. The composite material has a residual flux density of approximately 0.29 T and its storage modulus lies in the order of magnitude between 1 MPa and 10 MPa. After being exposed to a strong magnetic field, the composite remains magnetized, comparable to a stiff permanent magnet [16, 17].

Fig. 2a illustrates the flexibility of the H-MAE as well as its response to magnetic stimuli. A MAE beam is attached on the left end and deformed by the magnetic interactions with the magnet on the upper right side of the image. The geometric dimensions of the beams in the assembly are 60 mm × 6 mm × 3 mm (length × width × thickness). Both beams are magnetized in the direction of their thickness. In the assembly, they are stacked such as their magnetization points in the same direction (Fig. 2b). The magnetic attraction forces clamp the beams together and they stick to each other without the need for glue for the assembly.

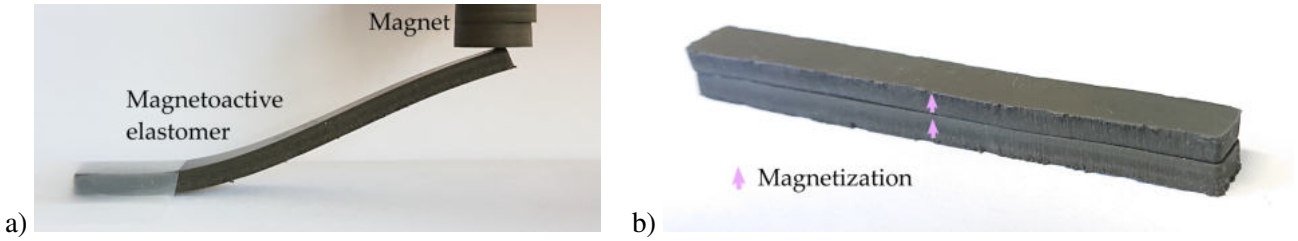

FIGURE 2 – Single magnetized H-MAE beam, attached on the left side and deformed by magnetic interactions with a magnet (a) and the magnetofriction shape memory polymer (MF-SMP) assembled from two magnetized H-MAE beams (b).

3 Storage of a deformed shape

3.1 Experimental setup and measurement protocol

Three-point bending tests are performed with the MF-SMP and one of the beams for comparison. The test rig is shown in Fig. 3. It is composed of a mechanical measurement setup, used to apply a loading and to measure the reaction forces, and an optic measurement setup used to record images for a digital image correlation (DIC). The specimens are positioned on the lower fixed part of the bending support in a dynamic mechanical analyzer. The displacement of the upper mobile part is controlled while the reaction force is measured with a unidirectional load cell, connected to the lower part (Fig. 4a). A lubricant is used to reduce the friction in the contact between the specimens and the bending test support.

The test is composed of different steps (cf. Fig. 4b) in order to evaluate the behavior of the specimens under different loading conditions. The tests starts by a first loading followed by a cyclic loading. Afterwards, five loading cycles with an amplitude of 1.5 mm are performed around an average displacement of 2 mm. A complete unloading is prevented since the reaction force can only be measured when the assembly is in contact with the mobile part of the testing machine. The displacement velocity is set to

0.12 mm/s. After the cyclic loading, the average displacement is maintained during five minutes. In the last step, the loading is removed.

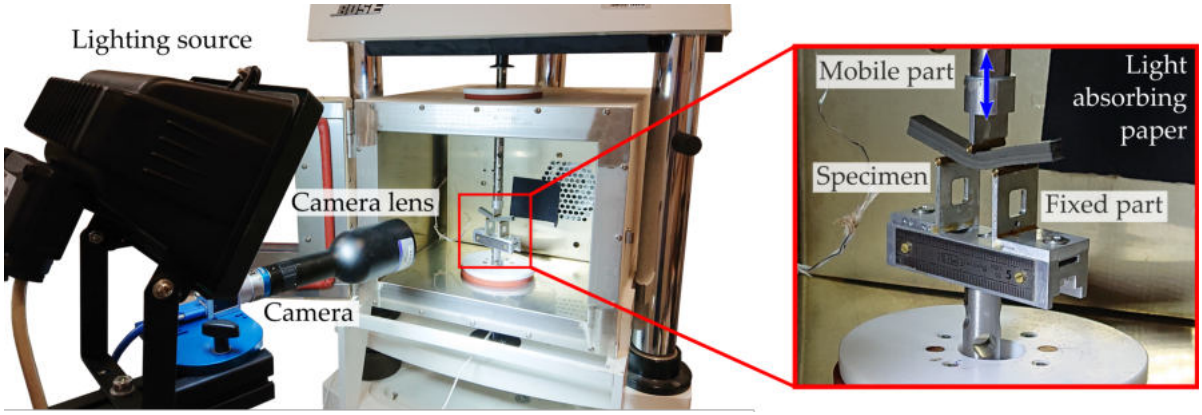

FIGURE 3 – Experimental setup for the three-point bending test.

The tests are filmed with a camera in order to perform the DIC later. The camera lens is arranged orthogonal to the specimen and points on the side of the assembly (Fig. 4a). An additional lighting source is used to improve the image quality. The light reflected by the metallic particles in the beam is sufficient to obtain a good contrast in the image which is important for the DIC. The images are recorded with a frequency of 2 Hz.

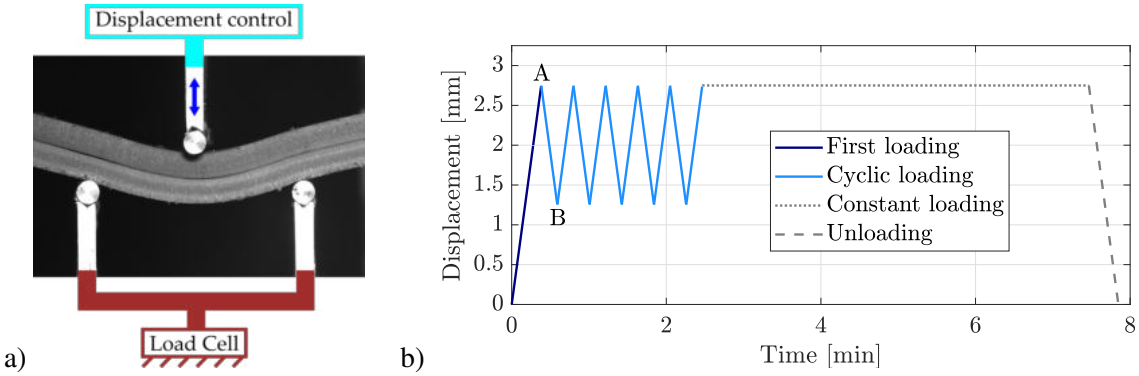

FIGURE 4 – Camera view of the MF-SMP in the experimental setup supplemented by schemes that illustrate the test configuration (a) and imposed displacement (a) highlighting the first loading and the subsequent five loading cycles blue.

The force and displacement data are obtained as text files from the machine and are converted from absolute to relative values during the post processing. For the digital image correlation, in-house algorithms are used to evaluate the camera images (.tiff). Boundaries and the contact interface are detected based on the contrast in the image (cf. Fig. 5). For the analysis of the local contact state, the position of regions of pixels has been traced by the help of a cross correlation that allows to recognize luminosity patterns.

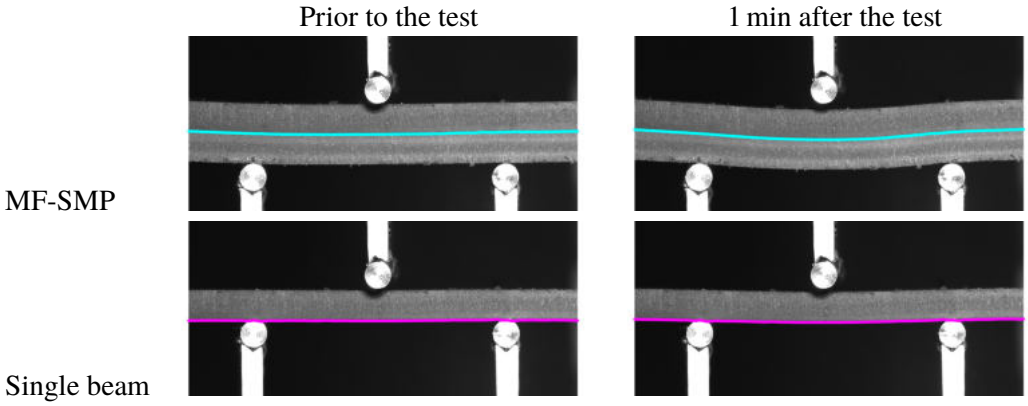

FIGURE 5 – Examples of the boundary detection : Interface of the MF-SMP (cyan) and boundary of the single beam (pink) detected in camera images taken before and after the mechanical loading.

3.2 Results

In the first study step, the stored displacements of the MF-SMP and the single beam are compared by the help of the detected boundaries. The displacement is calculated as the difference of the boundary positions before and after the test. Fig. 5 shows that both specimens remain deformed after the test and that the stored displacement is higher for the MF-SMP than for the single beam. Both specimens have a viscoelastic material behavior and are in contact with the experimental setup, where friction could provoke a residual displacement. The proof that magnetofriction is responsible for a part of the stored deformation in the MF-SMP is presented in the following.

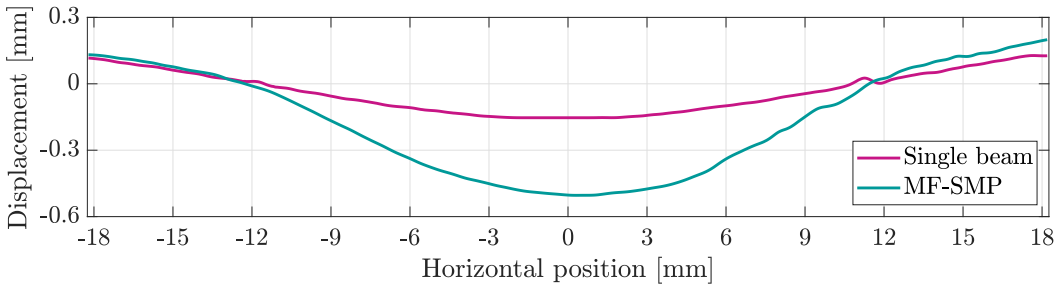

FIGURE 6 – Displacement of the interface in the MF-SMP and the lower boundary of the single beam 1 min after the test.

The reaction force of the specimens to the first loading and the subsequent five loading cycles is shown in Fig. 7. The elliptic shape of the loading cycles between the minimum and the maximum displacement (A and B, cf. Fig. 4) indicates a dissipative behavior of both specimens. A big difference between the specimens, however, is observed when the first loading is compared to the following loading cycles. The reaction force is almost similar for all loadings of the single beam. For the MF-SMP, the reaction force during the first loading is much higher than during the following cyclic loading.

The presence of magnetofriction can explain this behavior. During the first loading, the sticking threshold is exceeded in the contact interface and the beams start to slide over each other. A part of the constraints is released by the sliding. Due to the magnetic attraction forces, the beams stick together in a deformed shape. The force-displacement relations of the five loading cycles are similar, which indicates that the

loading is applied around a new, stabilized state. The existence of a stabilized state that persists after the test can explain the difference of the permanent deformation between the single beam and the MF-SMP after the test (Fig. 5). The evaluation of the local contact state confirms this hypothesis.

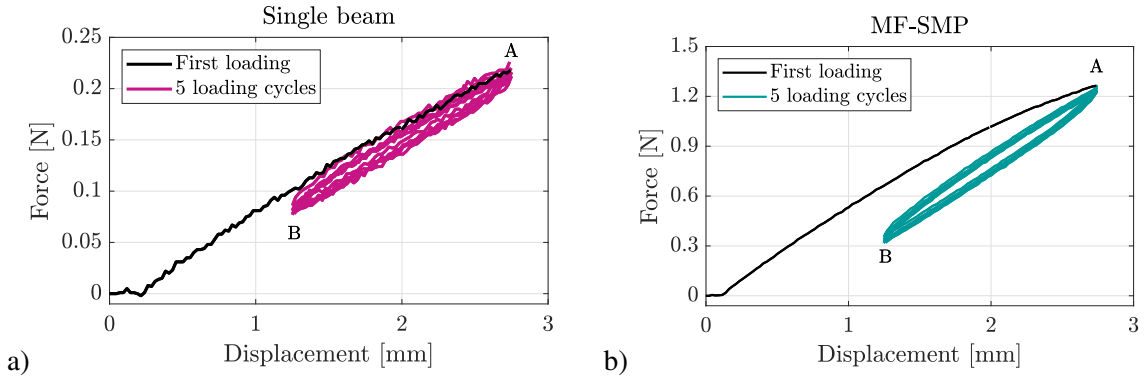

FIGURE 7 – Reaction force of the single beam (a) and the MF-SMP (b) for the first loading and the subsequent five loading cycles.

A region near the interface, in which both beams are visible, has been chosen for the evaluation. The region is highlighted by a red contour in the camera images (upper line) and the luminosity diagrams (lower line) of Fig. 8. The luminosity gradient is used to compare the relative positions of the upper and the lower beam for different steps of the experiment.

The lower image of Fig. 8a shows the evaluation region before the test. A pixel zone has been chosen in each beam for the tracing. Prior to the loading, the pixel zone in the upper beam (zone U) is located to the left of the pixel zone in the lower beam (zone L). When the first loading reaches its maximum (Fig. 8b), the zone U is now located to the right of the zone L. The sliding, which leads to the change of the relative positions is clearly visible in the intermediate images between the two states shown in Fig. 8a and Fig. 8b.

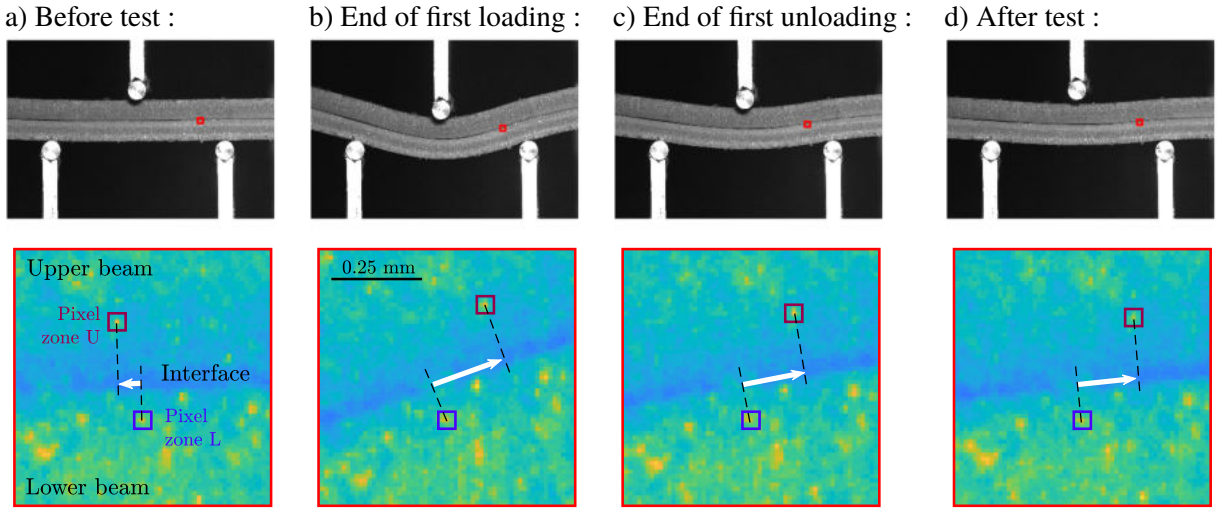

FIGURE 8 – Camera images (upper line) and luminosity diagrams in a small region of the beam (lower line) obtained before the test (a), after the first unloading phase (b, cf. Fig. 7b, point A), after the first unloading phase (c, cf. Fig. 7b, point B) and one minute after the test (d).

The distance between the pixel zones becomes slightly smaller after the first unloading but the zone U remains on the right side of the zone L (Fig. 8c). This results confirms the hypothesis from the previous paragraph : the beams slide over each other during the first loading but the deformed configuration remains stable during the cyclic loading. In addition, the pixel zones maintain their relative positions even after the unloading (Fig. 8d). The relative movement of the two beams has been observed in several regions of the MF-SMP which confirms that the deformed shape is obtained by magnetofriction.

4 Recovery of the initial shape

For the shape recovery of the MF-SMP, the contact pressure that generates the friction forces has to be suppressed. The easiest solutions for this is the separation of the two beams which is demonstrated in two simple tests. In a first step, the assembly is clamped in a cantilevered configuration (Fig. 9a), deformed manually (Fig. 9b) and does not deform back to its initial shape after being released (Fig. 9c).

a) Initial, stable state : b) Mechanical loading : c) Deformed, stable state :

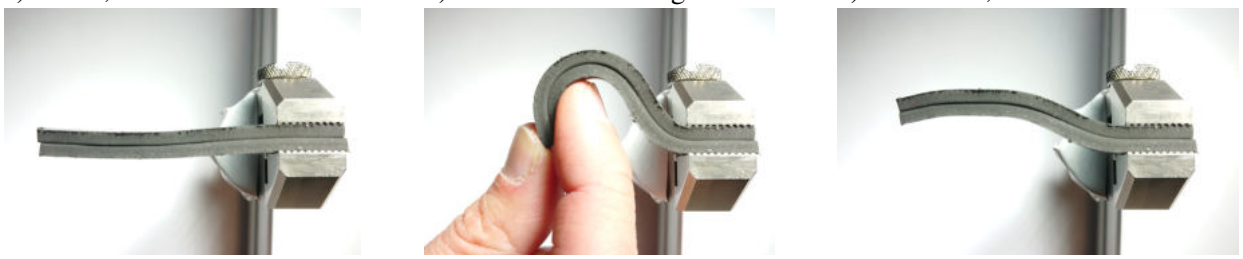

FIGURE 9 – Illustration of the deformation storage in the Magnetofriction Shape Memory Polymer (MF-SMP).

The separation can be performed manually (Fig. 10a). When the beams are brought near each other after the separation, the magnetic attraction forces restore the contact. Another possibility for the shape recovery is the a separation by an air flow between the beams (Fig. 10b). A tube is inserted in the clamping of the assembled structure and the air flow is strong enough to overcome the magnetic attraction forces between the beams. Due to the magnetic attraction forces, the beams stick together once the air flow is stopped.

a) b)

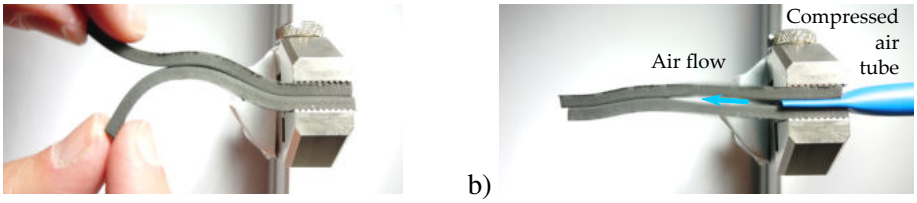

FIGURE 10 – Recovery of the initial shape by separation of the magnetized beams in the MF-SMP : manual separation of the beams (a) and separation of the beams by an air flow in the interface (b).

While the flexibility of the beams is an advantage for the deformation storage, it is a challenge for the recovery of the exact initial shape. Due to the magnetic forces, the beams attract each other when their distance is small enough. As a result, it is difficult to adjust the beams in their exact initial configuration after a separation of the beams. The restoring of the initial shape will hence be one of the challenges for future works.

5 Magnetofriction compared to other shape memory mechanisms

After the proof of the magnetofriction concept, the MF-SMP is now compared to common shape memory materials. As the concept is fairly new, it is a qualitative comparison that aims to position the new concept in the field of existing shape memory strategies. The comparison is detailed with reference to Tab. 1, in which different materials have been chosen to represent a shape memory mechanism.

In the MF-SMP, the effect is instantly activated when the adhesion threshold is exceeded in the contact interface. Concerning the time constant, it is more similar to the magnetically activated M-SMA and H-MAE than to thermally activated materials. The MF-SMP is therefore well suited for applications which require fast actuation cycles. The stiffness of the MF-SMP in its stable state lies below the stiffness of the SMA, the M-SMA and the SMP. It is comparable to the stiffness of H-MAE. Possible applications can therefore be found in similar fields like soft robotics or soft actuators for biomedical applications. In view of these application fields, the high shape change capacity of MF-SMP is an advantage. In contrast to H-MAE, MF-SMPs are capable to lock the shape of the deformed configuration without an external stimulus. H-MAEs remain deformed in a deformed shape only in presence of external magnetic fields. Therefore, MF-SMPs are favorable for applications in which stable states need to be maintained over a long time. While M-SMAs recover their initial shape the most precisely, the degree of shape recovery is slightly lower in the polymer materials.

The comparison of the different materials offers perspectives for future work on MF-SMP. Studies that quantify important aspects like the activation time or the stiffness variation during the transition could be performed. Additional important points for future studies are the magnetically induced contact pressure and the friction threshold in the MF-SMP.

TABLE 1 – Qualitative comparison of the properties of different shape memory alloys : Shape Memory Alloys (SMA), Shape Memory Polymers (SMP), Magnetic Shape Memory Alloys (M-SMA), Magnetic Shape Memory Elastomers (H-MAE) and the Magnetofriction Shape Memory Polymer (MF-SMP) of this work.

Criteria	**SMA**[6, 7]	**SMP**[18, 10]	**M-SMA**[19, 2]	**H-MAE** [14]	**MF-SMP**
Material	NiTi	Veriflex®	Ni-Mn-Ga	Silicone+NdFeB	Silicone+NdFeB
Activation type	Mechanics, Temperature	Mechanics, Temperature	Mechanics, Magnetism	Mechanics, Magnetism	Mechanics, Magnetism
Stiffness (ambient temperature)	●●●	●●○	●●●	●○○	●○○ [16]
Shape change capacity	●●●	●●●	●○○	●●○	●●○
Self-sufficient deformed state	✓	✓	✓	×	✓
Recovery of initial shape	●●●	●●○	●●●	●●○	●●○

6 Conclusions

This paper illustrates a new, multi-physical concept for shape memory in assembled structures which is called magnetofriction. The concept is based on the sliding in the interface between the assembled materials and governed by the competing strength of elastic forces and magnetically induced friction forces. An assembly of two magnetized H-MAE that form a magnetofriction Shape Memory Polymer (MF-SMP) is used for the experimental proof of concept. On a global scale, the storage of a deformed shape in bending tests is demonstrated. On a local scale, sliding in the interface is revealed by a digital image correlation. A manual separation and compressed air that temporarily flows through the interface are suggested as techniques for the recovery of the initial shape. The comparison of the new concept to common strategies for shape memory reveals possible application fields for magnetofriction and also helps to identify important aspects for future work on this topic.

Acknowledgments

This work has been funded by EIPHI Graduate School, ANR-17-EURE-0002.

Références

[1] M. Bengisu and M. Ferrara. *Materials that move : smart materials, intelligent design*. Springer, 2018.

[2] M. Kohl, M. Gueltig, V. Pinneker, R. Yin, F. Wendler, and B. Krevet. Magnetic shape memory microactuators. *Micromachines*, 5(4) :1135–1160, 2014.

[3] P. Motzki, F. Khelfa, L. Zimmer, M. Schmidt, and S. Seelecke. Design and validation of a reconfigurable robotic end-effector based on shape memory alloys. *IEEE/ASME Transactions on Mechatronics*, 24(1) :293–303, 2019.

[4] W. Hu, G. Z. Lum, M. Mastrangeli, and M. Sitti. Small-scale soft-bodied robot with multimodal locomotion. *Nature*, 554 :81–85, 2018.

[5] P.R. Buckley, T.S. McKinley, G.H. andWilson, W. Small, W.J. Bennett, J.P. Bearinger, M.W. McElfresh, and D.J. Maitland. Inductively heated shape memory polymer for the magnetic actuation of medical devices. *IEEE Trans. Biomed. Eng.*, 53 :2075—2083, 2006.

[6] K. Otsuka and C.M. Wayman. *Shape memory materials*. Cambridge university press, 1999.

[7] D.J. Hartl, D.C. Lagoudas, F.T. Calkins, and J.H. Mabe. Use of a ni60ti shape memory alloy for active jet engine chevron application : I. thermomechanical characterization. *Smart Materials and Structures*, 19(1) :015020, 2009.

[8] J. Diani, P. Gilormini, C. Frédy, and I. Rousseau. Predicting thermal shape memory of crosslinked polymer networks from linear viscoelasticity. *Int. J. Solids Struct.*, 49(5) :793—-799, 2012.

[9] P. Butaud, D. Renault, B. Verdin, M. Ouisse, and G. Chevallier. In-core heat distribution control for adaptive damping and stiffness tuning of composite structures. *Smart Materials and Structures*, 29(6) :065002, 2020.

[10] P. Butaud, V. Placet, J. Klesa, M. Ouisse, E. Foltête, and X. Gabrion. Investigations on the frequency and temperature effects on mechanical properties of a shape memory polymer (veriflex). *Mech. Mater.*, 87 :50—-60, 2015.

[11] A. M. Schmidt. Electromagnetic activation of shape memory polymer networks containing magnetic nanoparticles. *Macromolecular Rapid Communications*, 27(14) :1168–1172, 2006.

[12] Q. Ze, X. Kuang, S. Wu, J. Wong, S.M. Montgomery, R. Zhang, J.M. Kovitz, F. Yang, H.J. Qi, and R. Zhao. Magnetic shape memory polymers with integrated multifunctional shape manipulation. *Advanced Materials*, 32(4) :1906657, 2020.

[13] B. Kiefer and D.C. Lagoudas. Magnetic field-induced martensitic variant reorientation in magnetic shape memory alloys. *Philosophical Magazine*, pages 4289—-4329, 2005.

[14] Y. Kim, H. Yuk, R. Zhao, S.A. Chester, and X. Zhao. Printing ferromagnetic domains for untethered fast-transforming soft materials. *Nature*, 558 :274–291, 2018.

[15] S. Qi, H. Guo, J. Fu, Y. Xie, M. Zhu, and M. Yu. 3d printed shape-programmable magneto-active soft matter for biomimetic applications. *Composites Science and Technology*, 188 :107973, 2020.

[16] S. Hermann, P. Butaud, G. Chevallier, J.-F. Manceau, and C. Espanet. Magnetic and dynamic mechanical properties of a highly coercive mre based on ndfeb particles and a stiff matrix. *Smart Mater. Struct*, 29 :105009, 2020.

[17] S. Hermann, C. Espanet, P. Butaud, G. Chevallier, J.-F. Manceau, and L. Hirsinger. Modelization of the coupled behavior of a magnetically hard magnetoactive elastomer. In *Constitutive Moderls for Rubber XI*, pages 122–127. CRC Press, 2019.

[18] J. Ivens, M. Urbanus, and C. De Smet. Shape recovery in a thermoset shape memory polymer and its fabric-reinforced composites. *Express Polymer Letters*, 5(3) :254—-261, 2011.

[19] C. Segui, E. Cesari, J. Pons, and V. Chernenko. Internal friction behavior of Ni-Mn-Ga. *Materials Science and Engineering : A*, 73(1–2) :481–484, 2004.